

Resummed prediction for Higgs boson production through $b\bar{b}$ annihilation at $N^3\text{LO}+N^3\text{LL}$

Ajjath A H,^a Amlan Chakraborty,^a Goutam Das,^b Pooja Mukherjee,^a V. Ravindran^a

^a*The Institute of Mathematical Sciences, HBNI, IV Cross Road, Taramani, Chennai 600113, India*

^b*Theory Group, Deutsches Elektronen-Synchrotron (DESY), Notkestrasse 85, D-22607 Hamburg, Germany*

E-mail: ajjathah@imsc.res.in, amlanchak@imsc.res.in,

goutam.das@desy.de, poojamukherjee@imsc.res.in, ravindra@imsc.res.in

ABSTRACT: We present an accurate theoretical prediction for the production of Higgs boson through bottom quark annihilation at the LHC up to next-to-next-to-next-to leading order ($N^3\text{LO}$) plus next-to-next-to-next-to-leading logarithmic ($N^3\text{LL}$) accuracy. We determine the third order perturbative Quantum Chromodynamics (QCD) correction to the process dependent constant in the resummed expression using the three loop bottom quark form factor and third order quark soft distribution function. Thanks to the recent computation of $N^3\text{LO}$ corrections to this production cross section from all the partonic channels, an accurate matching can be obtained for a consistent predictions at $N^3\text{LO}+N^3\text{LL}$ accuracy in QCD. We have studied in detail the impact of resummed threshold contributions to inclusive cross sections at various centre of mass energy and also discussed their sensitivity to renormalisation and factorisation scales.

KEYWORDS: Resummation, Perturbative QCD

Contents

| | | |
|----------|--|-----------|
| 1 | Introduction | 1 |
| 2 | Theoretical Framework | 3 |
| 3 | Phenomenology | 6 |
| 4 | Conclusions | 11 |
| A | Resummation constants $g_i(\lambda, \mu_r^2, \mu_f^2)$ | 11 |
| B | Soft-Virtual coefficients in N-space | 13 |
| C | The Cusp and the soft anomalous dimensions | 15 |

1 Introduction

Discovery of the Higgs boson in 2012 is one of the biggest achievements of ATLAS [1] and CMS [2] collaborations at the Large Hadron Collider (LHC). It is a mile stone in the success of the Standard Model (SM). Having understood the generation of mass for the elementary particles through spontaneous symmetry breaking, it is important to understand the properties [3] of the Higgs boson such as spin, CP properties, self coupling and the couplings to the SM fermions and vector bosons. In the SM, Higgs boson is spin-0 and CP-even and it couples to SM fermions through Yukawa coupling. There exists several beyond the SM (BSM) scenarios which allow non SM spin-0 or spin-2 bosons to couple to SM particles. In addition, there exist CP mixing in the extended Higgs sectors. All these scenarios demonstrate distinct observable effects which can be studied at the LHC thereby constraining various BSM physics.

In recent years, efforts to understand the shape of the Higgs potential by measuring the Higgs self coupling in di-Higgs boson production is underway. It has important implications for the hierarchy problem, the vacuum metastability, the electroweak phase transition and baryogenesis. The measurement of the di-Higgs boson production at the LHC is plagued by the tiny cross section [4], however, the high luminosity option can help.

Yukawa couplings of the Higgs boson to the quarks and leptons of the SM are free parameters and hence, understanding their pattern is a great deal. As the mass of the Higgs boson is close to the electroweak scale, these couplings are highly sensitive to scales of new physics and measuring them precisely can probe various high scale physics scenarios. Both ATLAS [5] and CMS [6] collaborations have made dedicated efforts to measure them in various decay channels of the Higgs boson. Yukawa coupling of bottom quarks to the Higgs boson is one of the most sought parameter. However, measuring this coupling in the

dominant decay channel of the Higgs boson to a pair of bottom quarks is a challenging task. Associated production of Higgs boson with vector bosons or with top quarks, its subsequent decay to bottom quarks is the promising one while there are also other proposals [7].

While the Higgs boson dominantly decays to bottom quarks in SM, its production from bottom quark annihilation is much smaller than the gluon initiated subprocess. However, as the precise measurement of the Higgs cross sections is underway at the LHC, inclusion of bottom quark initiated channels in the theoretical predictions is unavoidable. Unlike in the SM, bottom quarks in the Minimal Supersymmetric SM (MSSM) [8] couple to neutral Higgs boson with the coupling proportional to $1/\cos\beta$ which in some parameter region can increase the production rate. Here, the angle β is related to the ratio, denoted by $\tan\beta$, of the vacuum expectation values of two Higgs doublets. Hence, there is a considerable interest in studying the production mechanism of a single and a pair of Higgs bosons through bottom quark annihilation. In the literature, the production of Higgs boson(s) is studied using two approaches namely four flavours and five flavour schemes often called 4FS and 5FS respectively. In 4FS, the bottom quark distribution in the proton is set equal to zero, however they are radiatively generated through gluons in the proton allowing the possibility of their annihilation to produce the Higgs boson. Such contributions are enhanced by logarithms that are sensitive to bottom quark mass and hence they need to be resummed to get reliable predictions. The alternative approach, 5FS, avoids this enhancement through the introduction of non-zero bottom quark distributions in the proton. The origin of these distributions can be traced back to the bottom quarks resulting from gluon distributions inside the proton, thanks to the DGLAP evolution equation of parton distribution functions, which resums collinear enhanced logarithms to all orders in perturbation theory. While both these schemes should give the same result at the observable level, care is needed while comparing their predictions. Since the leading order contribution to 4FS is two to three scattering reaction, while in 5FS, it is two to one, the higher order computations in perturbative Quantum Chromodynamics (QCD) in the later scheme is lot easier. Hence, till today, only next to leading order QCD effects [9–11] are known in 4FS while in 5FS, recently the state of the art N³LO prediction [12] is available. The later computation provides an opportunity to compare N³LO predictions against those at NLO computed in 4FS in a consistent manner. Note that, in 5FS, the complete NLO [13, 14] and NNLO [15] as well as dominant threshold effects at N³LO [16, 17] are known for quite sometime. In this article we improve the 5FS cross-section resumming threshold logarithms up to N³LL accuracy. The fact that the 5FS cross-section provides dominant cross-section in a matched prediction [18, 19] is very well known for quite a long. Thus threshold improved result justifies in the context of precision study for this process. Recently the 5FS prediction has been also improved [20] resumming time-like logarithms in SCET framework.

Fixed order predictions in perturbative QCD are often plagued with large logarithms resulting from certain boundaries of the phase space and hence their reliability in those regions are questionable. In the inclusive production rates, when partonic scaling variable $z = m_h^2/\hat{s} \rightarrow 1$, which corresponds to the emission of soft gluons, large logarithms are generated at every order in perturbation theory. Here, m_h is the Higgs boson mass and \hat{s} is the partonic centre of mass energy. One finds a similar problem in the transverse

momentum and rapidity distributions of Higgs boson when there are soft gluon emissions. This is resolved by resumming these large logs to all orders in perturbation theory through a systematic resummation approach. For inclusive rates, we refer [21–23] to the earliest approach. Catani and Trentadue, in their seminal work [22], demonstrated the resummation of leading large logs for the inclusive rates in Mellin space.

Needless to say that the inclusion of higher order QCD effects is of utmost importance to achieve precision prediction. In addition, these terms reduce the dependence on the unphysical scales such as renormalisation and factorisation at the observable level. Note that for the production of scalar Higgs boson through gluon fusion, the N³LO contribution is now known [24, 25], which was further improved by the resummation of threshold logarithms, arising from soft gluon emissions, to N³LL' accuracy [26–28] (the prime ' denotes that in addition to the N³LL terms the resummed result includes higher logarithmic order terms coming from the matching to N³LO). Such an analysis lead to a precise determination of the SM Higgs cross section at the LHC with small uncertainty.

The goal of the this paper is to present the prediction for the inclusive production of Higgs boson in bottom quark annihilation at the LHC taking into account the resummed threshold corrections at next-to-next-to-next to leading logarithmic accuracy. We can achieve this using the recent N³LO prediction [12] and N independent threshold constant $g_{b,0}$ computed to third order in QCD in this paper. Here, N denotes the Mellin moment. The $g_{b,0}^{(3)}$ is obtained using the three loop form factor [29] of the Higgs-bottom-anti bottom operator and the third order soft distribution function computed in [17].

2 Theoretical Framework

The Lagrangian that describes the Yukawa interaction of the SM Higgs boson with bottom quarks is given by

$$\mathcal{L}_{\text{int}}^{(S)} = -\lambda \bar{\psi}_b(x) \psi_b(x) \phi(x) \quad (2.1)$$

where $\psi_b(x)$ is the bottom quark field and $\phi(x)$ is the SM Higgs field. λ is the Yukawa coupling given by $\lambda = \frac{m_b}{v}$, where v is the vacuum expectation value of the Higgs field, m_b is the mass of the bottom quark. Note that we will use the non-zero mass of the bottom quark only in the Yukawa coupling, elsewhere it is treated as massless quarks i.e. we use the VFS scheme throughout our analysis. The inclusive cross-section for the production of Higgs boson in proton proton collision is given by

$$\sigma(\tau, m_h^2) = \tau \sigma_{bb}^{(0)}(\mu_r^2) \sum_{ab=q,\bar{q},g} \int \frac{dx_1}{x_1} \int \frac{dx_2}{x_2} f_a(x_1, \mu_f^2) f_b(x_2, \mu_f^2) \Delta_{ab} \left(\frac{\tau}{x_1 x_2}, \mu_r^2, \mu_f^2 \right) \quad (2.2)$$

where $f_c(x, \mu_f^2)$ is the non-perturbative parton distribution function with c denoting the parton type and x its momentum fraction, The scaling variable $\tau = m_h^2/S$ where S is the hadronic centre of mass energy. The renormalization and factorisation scales are denoted by μ_r and μ_f respectively. The born cross section $\sigma_{bb}^{(0)}(\mu_r^2)$ is given by

$$\sigma_{bb}^{(0)}(\mu_r^2) = \frac{\pi m_b^2(\mu_r^2)}{6m_h^2 v^2}. \quad (2.3)$$

The Δ_{ab} , mass factorised parton level cross section, is calculable order by order in strong coupling constant, $a_s(\mu_r^2) = g_s^2(\mu_r^2)/16\pi^2$ in perturbative QCD:

$$\Delta_{ab}(z, \mu_r^2, \mu_f^2) = \delta_{a\bar{b}}\delta(1-z) + \sum_{i=1}^{\infty} a_s^i(\mu_r^2) \Delta_{ab}^{(i)}(z, \mu_r^2, \mu_f^2) \quad (2.4)$$

At each order in perturbation theory we can write

$$\Delta_{ab}^{(i)}(z, \mu_r^2, \mu_f^2) = \delta_{a\bar{b}}\Delta^{SV,(i)}(z, \mu_r^2, \mu_f^2) + \Delta_{ab}^{reg,(i)}(z, \mu_r^2, \mu_f^2) \quad (2.5)$$

with $z = m_h^2/\hat{s}$. In the above equation Δ^{SV} collects all those contributions that result from soft and collinear configurations of partons in the scattering events. They are often proportional to distributions of the kind $\delta(1-z)$ and $\mathcal{D}_j(z)$ where

$$\mathcal{D}_j(z) = \left(\frac{\log^j(1-z)}{1-z} \right)_+, \quad j = 0, 1, 2, \dots \quad (2.6)$$

The superscript SV is the short form of soft plus virtual. The remaining contribution is called the regular part of the cross section denoted by Δ_{ab}^{reg} . In QCD, Δ_{ab} was computed up to NNLO level in [15], at N³LO level in the threshold limit it was obtained in [16, 17] and recently the complete N³LO result has been reported in [12].

The threshold contributions to inclusive cross section $\Delta_{ab}(z)$ originate from soft and collinear partons in the virtual and real emission subprocesses. These contributions demonstrate remarkable factorisation property through process independent cusp, soft and collinear anomalous dimensions. Consequently, the leading contributions resulting from the large threshold logarithms of the form $\mathcal{D}(z)$ can be summed to all orders in a systematic fashion. Following [21–23], the resummation of these logarithms can be efficiently achieved in Mellin N -space and the resulting resummed threshold contribution takes the following form:

$$\begin{aligned} \Delta_N^{res}(\mu_f^2) &= \int_0^1 dz \, z^{N-1} \Delta^{res}(z, \mu_f^2) \\ &= g_{b,0}(a_s(\mu_f^2)) \exp \left(\int_0^1 dz \frac{z^{N-1} - 1}{1-z} G_+(z, \mu_f^2) \right) \end{aligned} \quad (2.7)$$

where

$$G_+(z, \mu_f^2) = \left(\int_{\mu_f^2}^{q^2(1-z)^2} \frac{d\lambda^2}{\lambda^2} 2A^{(b)}(a_s(\lambda^2)) + D^{(b)}(a_s(q^2(1-z)^2)) \right)_+ \quad (2.8)$$

where we have set $\mu_r = \mu_f$. The cusp anomalous dimension $A^{(b)}(a_s)$ and the constant $D^{(b)}(a_s)$ are process independent and hence can be obtained from the resummation result of Drell-Yan process. They are known upto third order in QCD and are listed in the Appendix C. The N independent constant $g_{b,0}(a_s(\mu_f^2))$ on the other hand is process dependent. It gets contribution from the process dependent virtual Higgs-bottom-anti bottom quark form factor [29] and the soft distribution [16] resulting from real emission subprocesses.

We followed the method described in [16] (also see [30]) to obtain $g_{b,0}(a_s)$. Expanding $g_{b,0}(a_s(\mu_f^2))$ in powers of $a_s(\mu_r^2)$ as

$$g_{b,0}(a_s(\mu_f^2)) = 1 + \sum_{i=1}^{\infty} a_s^i(\mu_r^2) g_{b,0}^{(i)}(\mu_r^2, \mu_f^2) \quad (2.9)$$

we obtain up to three loop level

$$g_{b,0}^{(1)} = C_F \left\{ 16\zeta_2 + \left(-6 \right) L_{fr} - 4 \right\}, \quad (2.10)$$

$$\begin{aligned} g_{b,0}^{(2)} = & C_A C_F \left\{ -\frac{92}{5} \zeta_2^2 + \frac{256}{3} \zeta_2 + \frac{280}{9} \zeta_3 + \left(-\frac{88}{3} \zeta_2 - 24\zeta_3 - 12 \right) L_{qr} + \left(-\frac{88}{3} \zeta_2 + 24\zeta_3 \right. \right. \\ & \left. \left. - \frac{17}{3} \right) L_{fr} + \left(11 \right) L_{fr}^2 + \frac{166}{9} \right\} + C_F^2 \left\{ \frac{552}{5} \zeta_2^2 - 32\zeta_2 - 60\zeta_3 + \left(-72\zeta_2 - 48\zeta_3 \right. \right. \\ & \left. \left. + 21 \right) L_{fr} + \left(-24\zeta_2 + 48\zeta_3 \right) L_{qr} + \left(18 \right) L_{fr}^2 + 16 \right\} + C_F n_f \left\{ -\frac{40}{3} \zeta_2 + \frac{8}{9} \zeta_3 \right. \\ & \left. + \left(\frac{16}{3} \zeta_2 \right) L_{qr} + \left(\frac{16}{3} \zeta_2 + \frac{2}{3} \right) L_{fr} + \left(-2 \right) L_{fr}^2 + \frac{8}{9} \right\}, \end{aligned} \quad (2.11)$$

$$\begin{aligned} g_{b,0}^{(3)} = & C_A^2 C_F \left\{ \frac{7088}{63} \zeta_2^3 - \frac{25328}{135} \zeta_2^2 - \frac{7768}{9} \zeta_2 \zeta_3 + \frac{39980}{81} \zeta_2 - \frac{400}{3} \zeta_3^2 + \frac{42748}{81} \zeta_3 - 84\zeta_5 \right. \\ & \left. + \left(4\zeta_2^2 - \frac{8992}{27} \zeta_2 + \frac{3104}{9} \zeta_3 - 80\zeta_5 + \frac{1657}{18} \right) L_{fr} + \left(\frac{1964}{15} \zeta_2^2 - \frac{12800}{27} \zeta_2 - \frac{15472}{27} \zeta_3 \right. \right. \\ & \left. \left. + 80\zeta_5 - \frac{1180}{3} \right) L_{qr} + \left(\frac{968}{9} \zeta_2 - 88\zeta_3 + \frac{493}{9} \right) L_{fr}^2 + \left(\frac{968}{9} \zeta_2 + 88\zeta_3 + 44 \right) L_{qr}^2 + \left(\right. \right. \\ & \left. \left. - \frac{242}{9} \right) L_{fr}^3 + \frac{68990}{81} \right\} + C_A C_F^2 \left\{ -\frac{123632}{315} \zeta_2^3 + \frac{25676}{27} \zeta_2^2 + \frac{2528}{3} \zeta_2 \zeta_3 + \frac{19658}{27} \zeta_2 \right. \\ & \left. + \frac{592}{3} \zeta_3^2 - \frac{11188}{27} \zeta_3 - \frac{3352}{9} \zeta_5 + \left(-472\zeta_2^2 - 352\zeta_2 \zeta_3 - \frac{1748}{3} \zeta_2 + \frac{3296}{3} \zeta_3 + 240\zeta_5 \right. \right. \\ & \left. \left. + \frac{388}{3} \right) L_{qr} + \left(-\frac{1136}{5} \zeta_2^2 + 352\zeta_2 \zeta_3 - 212\zeta_2 - \frac{2536}{3} \zeta_3 - 240\zeta_5 - \frac{327}{2} \right) L_{fr} \right. \\ & \left. + \left(88\zeta_2 - 176\zeta_3 \right) L_{qr}^2 + \left(176\zeta_2 + 144\zeta_3 + 72 \right) L_{qr} L_{fr} + \left(264\zeta_2 + 32\zeta_3 + 1 \right) L_{fr}^2 \right. \\ & \left. + \left(-66 \right) L_{fr}^3 - \frac{982}{3} \right\} + C_A C_F n_f \left\{ \frac{184}{135} \zeta_2^2 + \frac{880}{9} \zeta_2 \zeta_3 - \frac{13040}{81} \zeta_2 - \frac{15944}{81} \zeta_3 - 8\zeta_5 \right. \\ & \left. + \left(-\frac{344}{15} \zeta_2^2 + \frac{4480}{27} \zeta_2 + \frac{3440}{27} \zeta_3 + \frac{196}{3} \right) L_{qr} + \left(-\frac{8}{5} \zeta_2^2 + \frac{2672}{27} \zeta_2 - \frac{400}{9} \zeta_3 \right. \right. \\ & \left. \left. - 40 \right) L_{fr} + \left(-\frac{352}{9} \zeta_2 - 16\zeta_3 - 8 \right) L_{qr}^2 + \left(-\frac{352}{9} \zeta_2 + 16\zeta_3 - \frac{146}{9} \right) L_{fr}^2 \right. \\ & \left. + \left(\frac{88}{9} \right) L_{fr}^3 - \frac{11540}{81} \right\} + C_F^3 \left\{ \frac{169504}{315} \zeta_2^3 - \frac{744}{5} \zeta_2^2 - 544\zeta_2 \zeta_3 - \frac{166}{3} \zeta_2 + 32\zeta_3^2 \right. \\ & \left. - 1188\zeta_3 + 848\zeta_5 + \left(-\frac{1968}{5} \zeta_2^2 - 704\zeta_2 \zeta_3 + 12\zeta_2 + 416\zeta_3 + 480\zeta_5 - 113 \right) L_{fr} + \left(\right. \right. \end{aligned}$$

$$\begin{aligned}
& -\frac{1344}{5}\zeta_2^2 + 704\zeta_2\zeta_3 + 132\zeta_2 - 56\zeta_3 - 480\zeta_5 - 100 \Big) L_{qr} + \left(144\zeta_2 - 288\zeta_3 \right) L_{qr} L_{fr} \\
& + \left(144\zeta_2 + 288\zeta_3 - 54 \right) L_{fr}^2 + \left(-36 \right) L_{fr}^3 + \frac{1078}{3} \Big\} + C_F^2 n_f \left\{ -\frac{15688}{135}\zeta_2^2 \right. \\
& - \frac{256}{3}\zeta_2\zeta_3 - \frac{3428}{27}\zeta_2 + \frac{8872}{27}\zeta_3 - \frac{608}{9}\zeta_5 + \left(\frac{272}{5}\zeta_2^2 + 56\zeta_2 + \frac{256}{3}\zeta_3 + 38 \right) L_{fr} \\
& + \left(\frac{464}{5}\zeta_2^2 + \frac{200}{3}\zeta_2 - \frac{656}{3}\zeta_3 + \frac{8}{3} \right) L_{qr} + \left(-48\zeta_2 - 32\zeta_3 - 4 \right) L_{fr}^2 + \left(\right. \\
& - 32\zeta_2 \Big) L_{qr} L_{fr} + \left(-16\zeta_2 + 32\zeta_3 \right) L_{qr}^2 + \left(12 \right) L_{fr}^3 - \frac{70}{9} \Big\} + C_F n_f^2 \left\{ \frac{448}{135}\zeta_2^2 \right. \\
& + \frac{256}{27}\zeta_2 + \frac{160}{81}\zeta_3 + \left(-\frac{320}{27}\zeta_2 - \frac{64}{27}\zeta_3 \right) L_{qr} + \left(-\frac{160}{27}\zeta_2 + \frac{32}{9}\zeta_3 + \frac{34}{9} \right) L_{fr} \\
& + \left(\frac{32}{9}\zeta_2 \right) L_{qr}^2 + \left(\frac{32}{9}\zeta_2 + \frac{4}{9} \right) L_{fr}^2 + \left(-\frac{8}{9} \right) L_{fr}^3 + \frac{16}{27} \Big\}, \tag{2.12}
\end{aligned}$$

where $C_A = N$ and $C_F = (N^2 - 1)/2N$ are the Casimirs of $SU(N)$ and $L_{fr} = \log(\mu_f^2/\mu_r^2)$ and $L_{qr} = \log(q^2/\mu_r^2)$. In addition ζ_i are the Riemann zeta functions.

Following the method described in [31], we have computed G_N to N³LL accuracy. Defining $\lambda = 2\beta_0 a(\mu_r^2) \ln(\bar{N})$, we obtain

$$\begin{aligned}
G_N &= \int_0^1 dz z^{N-1} G_+(z, \mu_f^2) \\
&= g_1(\lambda, \mu_r^2, \mu_f^2) \ln \bar{N} + \sum_{i=0}^{\infty} a_s^i(\mu_r^2) g_{i+2}(\lambda, \mu_r^2, \mu_f^2) \tag{2.13}
\end{aligned}$$

$\bar{N} = N \exp(\gamma_E)$ with $\gamma_E = 0.5772156649 \dots$, the Euler–Mascheroni constant. The successive terms in the above equation defines the resummation accuracy LL, NLL etc. Note that in the context of resummation, λ is of $\mathcal{O}(1)$. The resummation coefficients in Eq. (2.13) matches exactly with [31, 32] and for completeness we collect those in App. A.

Thus, the resummed contribution to the Higgs production in bottom quark annihilation in Mellin N -space takes the simple form

$$\Delta_N^{res}(\mu_r^2, \mu_f^2) = g_{b,0}(\mu_r^2, \mu_f^2) \exp(G_N(\lambda, \mu_r^2, \mu_f^2)) \tag{2.14}$$

The coefficients g_i for $i = 1, 2, 3, 4$ are listed in the Appendix. Note that except $A_4^{(b)}$ both the cusp $A^{(b)}$ and collinear $D^{(b)}$ anomalous dimensions are known to third order in a_s . Similarly $g_{b,0}$ is also known to order a_s^3 . Since the approximate $A_4^{(b)}$ is available in the literature we can readily predict N³LL contributions to inclusive Higgs production in bottom quark annihilation. In the next section, using the recently available predictions [12] for the fixed order N³LO contributions, we present the resummed prediction to N³LL + N³LO accuracy.

3 Phenomenology

In this section, we present a detailed discussion on the numerical impact of the resummed threshold contribution to the inclusive production of the Higgs boson in bottom quark

annihilation at the LHC up to N³LO+N³LL accuracy in perturbative QCD. The resummed part of the inclusive cross section for the Higgs production in N space can be obtained by taking N -th Mellin moment of Eq. (2.2) as

$$\sigma_{N-1}^{res} = \sigma_{bb}^{(0)}(\mu_r^2) \sum_{a=b, \bar{b}} f_{a,N}(\mu_f^2) f_{\bar{a},N}(\mu_f^2) \Delta_N^{res}(\mu_r^2, \mu_f^2) \quad (3.1)$$

where

$$\begin{aligned} \sigma_{N-1}^{res} &= \int_0^1 d\tau \tau^{N-2} \sigma^{res}(\tau, m_h^2), \\ f_{a,N} &= \int_0^1 dz z^{N-1} f_a(z, \mu_f^2). \end{aligned} \quad (3.2)$$

$\sigma^{res}(\tau, m_h^2)$ is the part of the cross section where $\Delta_{ab}(z, \mu_r^2, \mu_f^2)$ in Eq. (2.2) is replaced by $\Delta^{res}(z, \mu_r^2, \mu_f^2)$ whose N -th moment Δ_N^{res} is given in Eq. (2.7). The resummed cross section is then added to the fixed order one after subtracting the Mellin moment of $\Delta^{SV,(n)}(z)$ in the large N limit. This is done because they are already present in the fixed order result and hence this will avoid double counting. This is achieved through a matching procedure at every order. Finally, the matched result takes the following form:

$$\begin{aligned} \sigma^{N^n LO + N^n LL}(\tau, m_h^2) &= \sigma^{N^n LO}(\tau, m_h^2) + \sigma_{bb}^{(0)}(\mu_r^2) \int_{c-i\infty}^{c+i\infty} \frac{dN}{2\pi i} \left(\frac{m_h^2}{S} \right)^{-N+1} f_{b,N}(\mu_f^2) f_{\bar{b},N}(\mu_f^2) \\ &\times \left[\Delta_N^{res, N^n LL}(\mu_r^2, \mu_f^2) - \Delta_N^{res, N^n LL}(\mu_r^2, \mu_f^2) \Big|_{tr} \right]. \end{aligned} \quad (3.3)$$

In the above equation the superscript NⁿLL in Δ^{res} implies that we retain up to $g_{b,0}^{(n)}$ terms in the $g_{b,0}$ and up to $g_{n+1}(\lambda)$ in the exponent G_N given in Eq. (2.13). Similarly, NⁿLO implies that we retain the fixed order result up to order a_s^n . The subscript *tr* in the last term of the above equation means truncation of the series in a_s to desired accuracy.

The fixed order analytical results [15] up to NNLO order have been implemented in a fortran code. We have validated our predictions to a very good accuracy with the available public code SuShi [33]. For N³LO+N³LL analysis, we have used the numbers presented in Tab. II in the arXiv version of the paper [12] for N³LO. We perform the inverse Mellin transform of the resummed N -space result using an in-house fortran code. We have used the Minimal prescription [34] to deal with the Landau pole in the Mellin inversion routine.

Since we work in the 5FS, we take $n_f = 5$ throughout. We use the MMHT2014(68cl) PDF set [35] and renormalisation group (RG) running for a_s at each order. At N³LO + N³LL, we have used the four loop RG running for a_s , however for the PDF, we use NNLO set due to the unavailability of N³LO pdf sets. One could in principal use the strong coupling as provided through LHAPDF [36] interface, which at the NNLO level changes the cross-section by 0.09%. The Yukawa coupling is also evolved using 4 loop RG with bottom mass $m_b(m_b) = 4.3$ GeV. It is well known that the optimal choice for the central scale to study the Higgs production in bottom quark annihilation is $\mu_r = m_h$ and $\mu_f = m_h/4$. This choice mimics most of the higher order contributions. Hence, we have

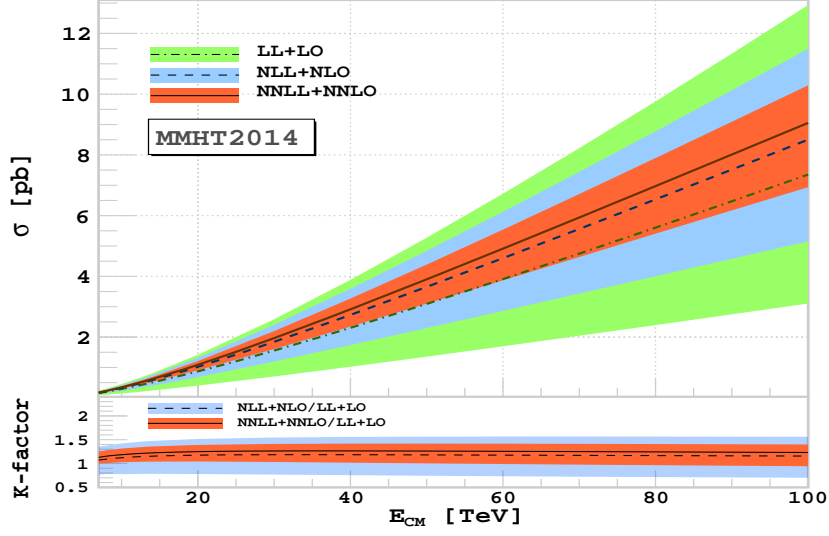


Figure 1. Resummed cross-section plotted against the hadronic centre-of-mass energy (E_{CM}). The band corresponds to the scale variation around the central scale choice $(\mu_r^{(c)}, \mu_f^{(c)}) = (1, 1/4)m_h$ along with the prediction for the central scale. In the lower inset the resummed K-factor has been shown along with scale uncertainties (see text).

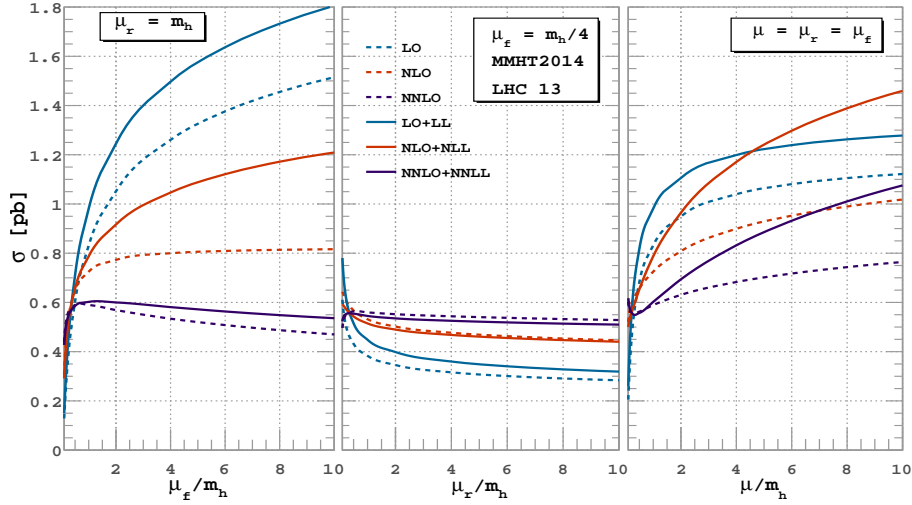


Figure 2. Fixed order and resummed cross-sections are plotted successively at each order up to NNLO level with unphysical factorisation (μ_f) scale varied in the range $(1/10, 10)m_h$ keeping renormalisation scale (μ_r) fixed at central value m_h . Similar variation for μ_r is done in the second panel keeping $\mu_f = m_h/4$. In the last panel, the μ_r is set to μ_f and is varied in the same range.

made this choice throughout. In addition, we have predictions for other central scale choice namely $\mu_r = \mu_f = m_h$.

In Fig. 1, we present the resummed cross-section up to NNLL+NNLO level against the

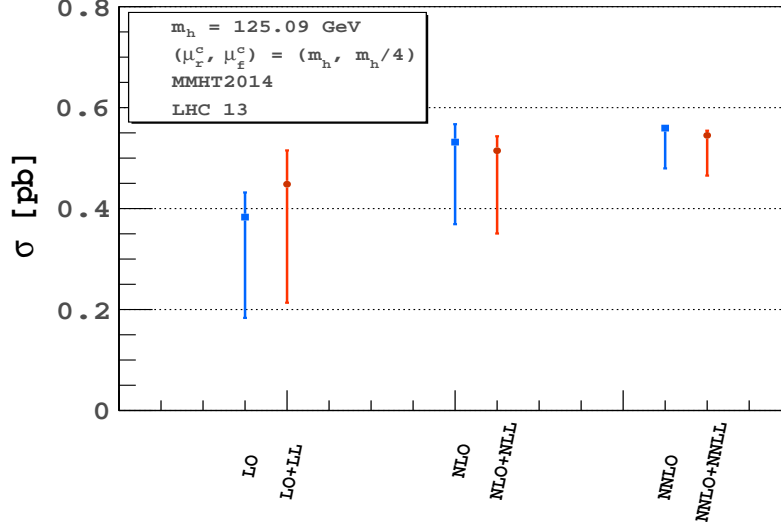


Figure 3. The perturbative convergence is shown for fixed order and resummed order for 13 TeV LHC. The central scale is fixed at $(1, 1/4)m_h$ and the asymmetric error bars are obtained by varying the μ_r, μ_f scales by $(1/2, 2)$ around their central scale.

| E_{CM} (TeV) | NNLO+NNLL (pb) | N ³ LO+N ³ LL (pb) |
|----------------|----------------|--|
| 7 | 0.174 | 0.172 |
| 8 | 0.225 | 0.223 |
| 13 | 0.535 | 0.536 |
| 14 | 0.605 | 0.608 |

Table 1. Resummed cross-sections are provided for 7, 8, 13, 14 TeV LHC with PDF4LHC2015nnlo pdf set for the central scale choice $(\mu_r^c, \mu_f^c) = (1, 1/4)m_h$.

hadronic centre-of-mass energy for 7 TeV to 100 TeV. The bands in the plot correspond to the scale variations obtained by varying the unphysical renormalisation and factorisation scales in the range $(1/2, 2)(\mu_r^{(c)}, \mu_f^{(c)})$ where the central scales are taken to be $(\mu_r^{(c)}, \mu_f^{(c)}) = (1, 1/4)m_h$. In the lower inset we show the corresponding resummed k -factors, defined as the ratio of the cross-section at a particular order (NLL+NLO, NNLL+NNLO) over the same at the LL+LO order. At NLL the k -factor increases by 14% and at NNLL by 21% compared to LL for 13 TeV LHC. We find that the uncertainty due to μ_r and μ_f scales increases with the energy of the collider, however at the current energy of the LHC it is within 11% at NNLL. The reason for the large uncertainty at high E_{CM} could be due to the lack of knowledge of the PDF sets at these energies

In Fig. 2, we study the sensitivity of our predictions to the renormalisation and factorisation scales at the LHC energy 13 TeV. For a conservative choice, we vary all the scales in the range $(0.1, 10)$, however in the later part of our analysis we followed the usual one in the range $(1/2, 2)$. For the μ_f variation (first panel), we have kept $\mu_r = m_h$ whereas for

the μ_r variation (second panel), we keep the factorisation scale to $\mu_f = m_h/4$. Finally in the third panel, we set $\mu_r = \mu_f = \mu$ and vary μ from $0.1m_h$ to $10m_h$. The cross-section decreases by 25% when μ_r is varied ten times its central value at LO. On the other hand it increases rapidly when μ_r is decreased and increases around 59% when the scale is taken one tenth of the central value. In the resum case the corresponding numbers are -28% and 74% respectively. At NLO level the fixed order cross-section changes by -16% to 21% whereas for NLO+NLL case it improves and changes by -14% to 15% . At the next order the corresponding numbers are -5% , 11% and -4.0% , 6.3% respectively. We observe that the resultant uncertainty from the renormalisation and factorisation scales after adding resummed result with the fixed one do not reduce significantly. This could be due to the fact that the resummation takes into account only the bottom quark initiated channels beyond $N^3\text{LO}$ accuracy. But the inclusion of the other channels can eventually lead to the reduction of the uncertainty. Moreover as we can see, the cross-section is particularly very sensitive to the μ_f variation even at NNLO level associated to the bottom quark pdf. A detailed analysis with respect to the choice of pdfs is thus required particularly how the underlying theoretical assumptions and models in the PDF fits affect the b-quark pdf determination [37].

At LO, the cross-section varies a lot with μ_f . However, at NNLO level, the uncertainty due to μ_f variation reduces to 15% whereas at NNLO+NNLL this goes down to 2%.

In Fig. 3, we compare the resummed cross-section against the fixed order one for 13 TeV LHC. The uncertainty is obtained using the 7-point variation i.e., by varying μ_r and μ_f scales around their central values m_h and $m_h/4$ respectively in the range $(1/2, 2)$.

At NNLL level the uncertainty is comparable to the corresponding fixed order result. However the central value of the resummed result shows a better perturbative convergence compared to the FO result. We find that the NLO cross-section increases by 38% compared to LO whereas NNLO increases by 5.2% compared to NLO. In the resummed case, the NLO+NLL cross-section increases by 14.8% compared to LO+LL result while NNLO+NNLL result increases by 5.8% compared to the NLO+NLL one at the central scale.

Recently, the complete result for Δ_{ab} to third order, namely $\Delta_{ab}^{(3)}$ s have become available [12] and this allows us to predict the matched cross section to $N^3\text{LO}+N^3\text{LL}$ accuracy. We have used same set of input parameters as in [12] for our study. In particular, we have used the PDF4LHC2015nnlo set with strong coupling evolved at four loops. The bottom quark mass is taken to be $m_b(m_b) = 4.18$ GeV. At the LHC energy 13 TeV we find that the $N^3\text{LO}$ SV cross-section deviates from the complete $N^3\text{LO}$ result by around 2%. Our prediction for the cross-section at the central scale at $N^3\text{LO}+N^3\text{LL}$ level is 0.537 pb which changes the fixed order cross-section by around -1% . The renormalisation and factorisation scale dependence can also be studied for the matched cross section, once their code [12] is publicly available. However, we expect the scale variation at this order will be negligible and the dominant uncertainty will come from the PDF errors which can be addressed when $N^3\text{LO}$ pdfs become available.

In Table-1 we quote the prediction at NNLO+NNLL and $N^3\text{LO}+N^3\text{LL}$ level for the central scale choice $(\mu_r^c, \mu_f^c) = (1, 1/4)m_h$ for centre-of-mass energies 7, 8, 13 and 14 TeV.

We find that the central scale choice stabilises for different collider energies already at NNLO+NNLL level. At N³LO+N³LL level, the change is well within 0.2%.

4 Conclusions

In this article we have studied the role of resummed threshold corrections to the inclusive cross section for producing the Higgs boson through bottom quark annihilation at the LHC. While this is a sub-dominant channel compared to gluon fusion subprocess, the precise measurements that are carried out at the LHC in the context of processes involving Higgs bosons demand the inclusion of this channel for the precision studies. Complete NNLO QCD corrections [15] and soft plus virtual corrections [17] to N³LO level to this observable are known for a while. More recently, a complete N³LO contributions resulting from all the partonic channels where the Higgs boson couples to bottom quarks became available [12]. In hadronic colliders, soft gluons play important role in most of the observables. In the fixed order perturbative computations, in certain kinematic regions the soft gluons dominate. The large logarithms resulting from these soft gluons often spoil the reliability of the fixed order predictions. The resolution to this problem is to resum these logarithms to all orders in perturbation theory. The framework to resum such logarithms in a systematic fashion to all orders in perturbation theory for inclusive observables is well established and results based on this demonstrate better and reliable predictions compared to the fixed order ones. In the present article we have done a detailed study to understand the role of the soft gluons on the inclusive cross section for producing Higgs boson in bottom quark annihilation. This is achieved within the frame work of threshold resummation in Mellin-N space. We have done this to N³LO+N³LL accuracy. We have used the recent prediction at N³LO level from [12] for the fixed order contribution and for the resummed part at N³LL level, except the process dependent constant $g_{b0}^{(3)}$, rest of the ingredients are already known. We have computed this constant for the first time using the three loop form factor [29] and the quark soft distribution function [17] known to third order in QCD. Our numerical result at N³LO+N³LL in QCD is the most precise prediction for the inclusive cross section for the production of Higgs boson through bottom quarks at the LHC. We have predicted the inclusive rates at various centre of mass energies with the corresponding k -factors. In addition, we studied in detail the sensitivity of the resummed predictions to the renormalisation and factorisation scales in order to estimate the theoretical errors precisely.

Acknowledgements

We would like to thank P. K. Dhani for initial collaboration. We also thank S. Moch, F. J. Tackmann and J. K. L. Michel for useful discussions.

A Resummation constants $g_i(\lambda, \mu_r^2, \mu_f^2)$

$$g_1 = \left[\frac{A_1^{(b)}}{\beta_0} \left\{ 2 - 2 \ln(1 - \lambda) + 2 \ln(1 - \lambda) \lambda^{-1} \right\} \right], \quad (\text{A.1})$$

$$g_2 = \left[\frac{D_1^{(b)}}{\beta_0} \left\{ \frac{1}{2} \ln(1-\lambda) \right\} + \frac{A_2^{(b)}}{\beta_0^2} \left\{ -\ln(1-\lambda) - \lambda \right\} + \frac{A_1^{(b)}}{\beta_0} \left\{ \left(\ln(1-\lambda) + \frac{1}{2} \ln(1-\lambda)^2 + \lambda \right) \left(\frac{\beta_1}{\beta_0^2} \right) + \left(\lambda \right) L_{fr} + \left(\ln(1-\lambda) \right) L_{qr} \right\} \right], \quad (\text{A.2})$$

$$g_3 = \left[\frac{A_3^{(b)}}{\beta_0^2} \left\{ \frac{1}{2} \frac{\lambda}{(1-\lambda)} - \frac{1}{2} \lambda \right\} + \frac{A_2^{(b)}}{\beta_0} \left\{ \left(-\frac{3}{2} \frac{\lambda}{(1-\lambda)} - \frac{\ln(1-\lambda)}{(1-\lambda)} + \frac{1}{2} \lambda \right) \left(\frac{\beta_1}{\beta_0^2} \right) + \left(-\frac{\lambda}{(1-\lambda)} \right) L_{qr} + \left(\lambda \right) L_{fr} \right\} + A_1^{(b)} \left\{ 2 \zeta_2 \frac{\lambda}{(1-\lambda)} + \left(\frac{1}{2} \frac{\ln(1-\lambda)^2}{(1-\lambda)} + \frac{1}{2} \frac{\lambda}{(1-\lambda)} + \frac{\ln(1-\lambda)}{(1-\lambda)} - \ln(1-\lambda) - \frac{1}{2} \lambda \right) \left(\frac{\beta_1}{\beta_0^2} \right)^2 + \left(\frac{1}{2} \frac{\lambda}{(1-\lambda)} \right) L_{qr}^2 + \left(\frac{1}{2} \frac{\lambda}{(1-\lambda)} + \ln(1-\lambda) + \frac{1}{2} \lambda \right) \left(\frac{\beta_2}{\beta_0^3} \right) + \left(-\frac{1}{2} \lambda \right) L_{fr}^2 + \left(\left(\frac{\lambda}{(1-\lambda)} + \frac{\ln(1-\lambda)}{(1-\lambda)} \right) \left(\frac{\beta_1}{\beta_0^2} \right) \right) L_{qr} \right\} + \frac{D_2^{(b)}}{\beta_0} \left\{ -\frac{1}{2} \frac{\lambda}{(1-\lambda)} \right\} + D_1^{(b)} \left\{ \left(\frac{1}{2} \frac{\lambda}{(1-\lambda)} \right) L_{qr} + \left(\frac{1}{2} \frac{\lambda}{(1-\lambda)} + \frac{1}{2} \frac{\ln(1-\lambda)}{(1-\lambda)} \right) \left(\frac{\beta_1}{\beta_0^2} \right) \right\} \right], \quad (\text{A.3})$$

$$g_4 = \left[\frac{A_4^{(b)}}{\beta_0^2} \left\{ \frac{1}{6} \frac{\lambda(2-\lambda)}{(1-\lambda)^2} - \frac{1}{3} \lambda \right\} + \frac{A_3^{(b)}}{\beta_0} \left\{ \left(-\frac{1}{2} \frac{\lambda(2-\lambda)}{(1-\lambda)^2} \right) L_{qr} + \left(-\frac{5}{12} \frac{\lambda(2-\lambda)}{(1-\lambda)^2} - \frac{1}{2} \frac{\ln(1-\lambda)}{(1-\lambda)^2} + \frac{1}{3} \lambda \right) \left(\frac{\beta_1}{\beta_0^2} \right) + \left(\lambda \right) L_{fr} \right\} + A_2^{(b)} \left\{ 2 \zeta_2 \frac{\lambda(2-\lambda)}{(1-\lambda)^2} + \left(\frac{1}{2} \frac{\ln(1-\lambda)^2}{(1-\lambda)^2} - \frac{1}{12} \frac{\lambda^2}{(1-\lambda)^2} + \frac{5}{6} \frac{\lambda}{(1-\lambda)} + \frac{1}{2} \frac{\ln(1-\lambda)}{(1-\lambda)^2} - \frac{1}{3} \lambda \right) \left(\frac{\beta_1}{\beta_0^2} \right)^2 + \left(\frac{1}{2} \frac{\lambda(2-\lambda)}{(1-\lambda)^2} \right) L_{qr}^2 + \left(\frac{1}{3} \frac{\lambda^2}{(1-\lambda)^2} - \frac{1}{3} \frac{\lambda}{(1-\lambda)} + \frac{1}{3} \lambda \right) \left(\frac{\beta_2}{\beta_0^3} \right) + \left(-\lambda \right) L_{fr}^2 + \left(\left(\frac{1}{2} \frac{\lambda(2-\lambda)}{(1-\lambda)^2} + \frac{\ln(1-\lambda)}{(1-\lambda)^2} \right) \left(\frac{\beta_1}{\beta_0^2} \right) \right) L_{qr} \right\} + \beta_0 A_1^{(b)} \left\{ \frac{8}{3} \zeta_3 \frac{\lambda(2-\lambda)}{(1-\lambda)^2} + \left(-\frac{1}{6} \frac{\ln(1-\lambda)^3}{(1-\lambda)^2} + \frac{1}{3} \frac{\lambda^2}{(1-\lambda)^2} - \frac{1}{3} \frac{\lambda}{(1-\lambda)} + \frac{1}{2} \frac{\ln(1-\lambda)}{(1-\lambda)^2} - \frac{\ln(1-\lambda)}{(1-\lambda)} + \frac{1}{2} \ln(1-\lambda) + \frac{1}{3} \lambda \right) \left(\frac{\beta_1}{\beta_0^2} \right)^3 + \left(-\frac{1}{6} \frac{\lambda(2-\lambda)}{(1-\lambda)^2} \right) L_{qr}^3 + \left(\frac{1}{12} \frac{\lambda(2-\lambda)}{(1-\lambda)^2} + \frac{1}{2} \ln(1-\lambda) + \frac{1}{3} \lambda \right) \left(\frac{\beta_3}{\beta_0^4} \right) + \left(-\frac{5}{12} \frac{\lambda^2}{(1-\lambda)^2} + \frac{1}{6} \frac{\lambda}{(1-\lambda)} - \frac{1}{2} \frac{\ln(1-\lambda)}{(1-\lambda)^2} + \frac{\ln(1-\lambda)}{(1-\lambda)} - \ln(1-\lambda) - \frac{2}{3} \lambda \right) \frac{\beta_1 \beta_2}{\beta_0^5} + \left(\frac{1}{3} \lambda \right) L_{fr}^3 + \left(-2 \zeta_2 \frac{\lambda(2-\lambda)}{(1-\lambda)^2} + \left(-\frac{1}{2} \frac{\ln(1-\lambda)^2}{(1-\lambda)^2} + \frac{1}{2} \frac{\lambda^2}{(1-\lambda)^2} \right) \left(\frac{\beta_1}{\beta_0^2} \right)^2 + \left(-\frac{1}{2} \frac{\lambda^2}{(1-\lambda)^2} \right) \left(\frac{\beta_2}{\beta_0^3} \right) \right) L_{qr} + \left(-2 \zeta_2 \frac{\ln(1-\lambda)}{(1-\lambda)^2} \right) \left(\frac{\beta_1}{\beta_0^2} \right) + \left(\left(-\frac{1}{2} \frac{\ln(1-\lambda)}{(1-\lambda)^2} \right) \left(\frac{\beta_1}{\beta_0^2} \right) \right) L_{qr}^2 + \left(\left(-\frac{1}{2} \lambda \right) \left(\frac{\beta_1}{\beta_0^2} \right) \right) L_{fr}^2 \right\} + \frac{D_3^{(b)}}{\beta_0} \left\{ -\frac{1}{4} \frac{\lambda(2-\lambda)}{(1-\lambda)^2} \right\} + D_2^{(b)} \left\{ \left(\frac{1}{4} \frac{\lambda(2-\lambda)}{(1-\lambda)^2} + \frac{1}{2} \frac{\ln(1-\lambda)}{(1-\lambda)^2} \right) \left(\frac{\beta_1}{\beta_0^2} \right) + \left(\frac{1}{2} \frac{\lambda(2-\lambda)}{(1-\lambda)^2} \right) L_{qr} \right\} + \beta_0 D_1^{(b)} \left\{ \right.$$

$$\begin{aligned}
& -\zeta_2 \frac{\lambda(2-\lambda)}{(1-\lambda)^2} + \left(-\frac{1}{4} \frac{\ln(1-\lambda)^2}{(1-\lambda)^2} + \frac{1}{4} \frac{\lambda^2}{(1-\lambda)^2} \right) \left(\frac{\beta_1}{\beta_0^2} \right)^2 + \left(-\frac{1}{4} \frac{\lambda(2-\lambda)}{(1-\lambda)^2} \right) L_{qr}^2 \\
& + \left(-\frac{1}{4} \frac{\lambda^2}{(1-\lambda)^2} \right) \left(\frac{\beta_2}{\beta_0^3} \right) + \left(\left(-\frac{1}{2} \frac{\ln(1-\lambda)}{(1-\lambda)^2} \right) \left(\frac{\beta_1}{\beta_0^2} \right) \right) L_{qr} \Bigg], \tag{A.4}
\end{aligned}$$

B Soft-Virtual coefficients in N -space

Here we have collected all the large N coefficients for this process. Defining $\bar{L} = \ln N + \gamma_E$ they are given below:

$$\Delta_{sv}^{(1)} = \bar{L}^2 \left\{ \binom{8}{8} C_F \right\} + \bar{L} \left\{ \left(\binom{-8}{8} L_{qr} + \binom{8}{8} L_{fr} \right) C_F \right\} + g_{01}, \tag{B.1}$$

$$\begin{aligned}
\Delta_{sv}^{(2)} = & \bar{L}^4 \left\{ \binom{32}{32} C_F^2 \right\} + \bar{L}^3 \left\{ \left(\binom{-64}{64} L_{qr} + \binom{64}{64} L_{fr} \right) C_F^2 + \left(-\frac{32}{9} \right) C_F n_f \right. \\
& + \left. \left(\frac{176}{9} \right) C_A C_F \right\} + \bar{L}^2 \left\{ \left(-16\zeta_2 + \left(-\frac{88}{3} \right) L_{qr} + \frac{536}{9} \right) C_A C_F + \left(128\zeta_2 \right. \right. \\
& + \left. \left(-64 \right) L_{qr} L_{fr} + \left(-48 \right) L_{fr} + \left(32 \right) L_{qr}^2 + \left(32 \right) L_{fr}^2 - 32 \right) C_F^2 + \left(\left(\frac{16}{3} \right) L_{qr} \right. \\
& - \left. \frac{80}{9} \right) C_F n_f \Bigg\} + \bar{L} \left\{ \left(-56\zeta_3 + \left(-16\zeta_2 + \frac{536}{9} \right) L_{fr} + \left(16\zeta_2 - \frac{536}{9} \right) L_{qr} + \left(\right. \right. \right. \\
& - \left. \left. \frac{44}{3} \right) L_{fr}^2 + \left(\frac{44}{3} \right) L_{qr}^2 + \frac{1616}{27} \right) C_A C_F + \left(\left(-128\zeta_2 + 32 \right) L_{qr} + \left(128\zeta_2 \right. \right. \\
& - \left. \left. 32 \right) L_{fr} + \left(-48 \right) L_{fr}^2 + \left(48 \right) L_{qr} L_{fr} \right) C_F^2 + \left(\left(-\frac{80}{9} \right) L_{fr} + \left(-\frac{8}{3} \right) L_{qr}^2 \right. \\
& + \left. \left(\frac{8}{3} \right) L_{fr}^2 + \left(\frac{80}{9} \right) L_{qr} - \frac{224}{27} \right) C_F n_f \Bigg\} + g_{02}, \tag{B.2}
\end{aligned}$$

$$\begin{aligned}
\Delta_{sv}^{(3)} = & \bar{L}^6 \left\{ \left(\frac{256}{3} \right) C_F^3 \right\} + \bar{L}^5 \left\{ \left(\binom{-256}{256} L_{qr} + \binom{256}{256} L_{fr} \right) C_F^3 + \left(-\frac{256}{9} \right) C_F^2 n_f \right. \\
& + \left. \left(\frac{1408}{9} \right) C_A C_F^2 \right\} + \bar{L}^4 \left\{ \left(-128\zeta_2 + \left(-\frac{3520}{9} \right) L_{qr} + \left(\frac{1408}{9} \right) L_{fr} \right. \right. \\
& + \left. \left. \frac{4288}{9} \right) C_A C_F^2 + \left(512\zeta_2 + \left(-512 \right) L_{qr} L_{fr} + \left(-192 \right) L_{fr} + \left(256 \right) L_{qr}^2 \right. \right. \\
& + \left. \left. \left(256 \right) L_{fr}^2 - 128 \right) C_F^3 + \left(\left(-\frac{256}{9} \right) L_{fr} + \left(\frac{640}{9} \right) L_{qr} - \frac{640}{9} \right) C_F^2 n_f + \left(\right. \right. \\
& - \left. \left. \frac{704}{27} \right) C_A C_F n_f + \left(\frac{64}{27} \right) C_F n_f^2 + \left(\frac{1936}{27} \right) C_A^2 C_F \right\} + \bar{L}^3 \left\{ \left(-\frac{704}{9} \zeta_2 + \left(\right. \right. \right. \\
& - \left. \left. \frac{3872}{27} \right) L_{qr} + \frac{28480}{81} \right) C_A^2 C_F + \left(-\frac{512}{9} \zeta_2 + \left(-\frac{1088}{9} \right) L_{fr} + \left(\frac{64}{3} \right) L_{fr}^2 \right. \\
& + \left(\frac{128}{3} \right) L_{qr} L_{fr} + \left(\frac{1280}{9} \right) L_{qr} + \left(-64 \right) L_{qr}^2 - \frac{1696}{27} \right) C_F^2 n_f + \left(\frac{128}{9} \zeta_2 \right. \\
& + \left. \left(\frac{1408}{27} \right) L_{qr} - \frac{9248}{81} \right) C_A C_F n_f + \left(\frac{2816}{9} \zeta_2 - 448\zeta_3 + \left(-256\zeta_2 + \frac{7520}{9} \right) L_{fr} \right.
\end{aligned}$$

$$\begin{aligned}
& + \left(256\zeta_2 - \frac{8576}{9}\right)L_{qr} + \left(-\frac{704}{3}\right)L_{qr}L_{fr} + \left(-\frac{352}{3}\right)L_{fr}^2 + \left(352\right)L_{qr}^2 \\
& + \frac{10816}{27}C_A C_F^2 + \left(\left(-1024\zeta_2 + 256\right)L_{qr} + \left(1024\zeta_2 - 256\right)L_{fr} + \left(-\frac{256}{3}\right)L_{qr}^3\right. \\
& + \left(\frac{256}{3}\right)L_{fr}^3 + \left(-384\right)L_{fr}^2 + \left(-256\right)L_{qr}L_{fr}^2 + \left(256\right)L_{qr}^2L_{fr} \\
& + \left(384\right)L_{qr}L_{fr}\left.C_F^3 + \left(\left(-\frac{128}{27}\right)L_{qr} + \frac{640}{81}\right)C_F n_f^2\right\} + \bar{L}^2\left\{\left(-\frac{2016}{5}\zeta_2^2\right.\right. \\
& + \frac{15296}{9}\zeta_2 + \frac{2240}{9}\zeta_3 + \left(-704\zeta_2 + 256\zeta_3 - \frac{12352}{27}\right)L_{qr} + \left(-\frac{416}{3}\zeta_2 - 256\zeta_3\right. \\
& + \frac{2056}{27}\left.)L_{fr} + \left(-128\zeta_2 + \frac{4288}{9}\right)L_{qr}^2 + \left(-128\zeta_2 + \frac{5080}{9}\right)L_{fr}^2 + \left(256\zeta_2\right.\right. \\
& - \frac{6992}{9}\left.)L_{qr}L_{fr} + \left(-\frac{352}{3}\right)L_{qr}^3 + \left(-\frac{352}{3}\right)L_{fr}^3 + \left(\frac{352}{3}\right)L_{qr}^2L_{fr} \\
& + \left(\frac{352}{3}\right)L_{qr}L_{fr}^2 - \frac{272}{3}\left.)C_A C_F^2 + \left(\frac{352}{5}\zeta_2^2 - \frac{2144}{9}\zeta_2 - 352\zeta_3 + \left(\frac{352}{3}\zeta_2\right.\right.\right. \\
& - \frac{14240}{27}\left.)L_{qr} + \left(\frac{968}{9}\right)L_{qr}^2 + \frac{62012}{81}\left.)C_A^2 C_F + \left(\frac{4416}{5}\zeta_2^2 - 256\zeta_2 - 480\zeta_3 + \left(-1024\zeta_2 + 256\right)L_{qr}L_{fr} + \left(-576\zeta_2 - 384\zeta_3 + 168\right)L_{fr} + \left(-192\zeta_2 + 384\zeta_3\right)L_{qr}\right.\right. \\
& + \left(512\zeta_2 - 128\right)L_{qr}^2 + \left(512\zeta_2 + 16\right)L_{fr}^2 + \left(-192\right)L_{fr}^3 + \left(-192\right)L_{qr}^2L_{fr} \\
& + \left(384\right)L_{qr}L_{fr}^2 + 128\left.)C_F^3 + \left(-\frac{2240}{9}\zeta_2 + \frac{640}{9}\zeta_3 + \left(\frac{128}{3}\zeta_2 - \frac{208}{27}\right)L_{fr}\right.\right. \\
& + \left(128\zeta_2 + \frac{1648}{27}\right)L_{qr} + \left(-\frac{784}{9}\right)L_{fr}^2 + \left(-\frac{640}{9}\right)L_{qr}^2 + \left(-\frac{64}{3}\right)L_{qr}^2L_{fr} + \left(-\frac{64}{3}\right)L_{qr}L_{fr}^2 + \left(\frac{64}{3}\right)L_{qr}^3 + \left(\frac{64}{3}\right)L_{fr}^3 + \left(\frac{992}{9}\right)L_{qr}L_{fr} - \frac{92}{3}\left.)C_F^2 n_f + \left(\frac{320}{9}\zeta_2\right.\right. \\
& + \left(-\frac{64}{3}\zeta_2 + \frac{4624}{27}\right)L_{qr} + \left(-\frac{352}{9}\right)L_{qr}^2 - \frac{16408}{81}\left.)C_A C_F n_f + \left(\left(-\frac{320}{27}\right)L_{qr}\right.\right. \\
& + \left(\frac{32}{9}\right)L_{qr}^2 + \frac{800}{81}\left.)C_F n_f^2\right\} + \bar{L}\left\{\left(-\frac{176}{5}\zeta_2^2 + \frac{352}{3}\zeta_2\zeta_3 - \frac{12784}{81}\zeta_2 - \frac{24656}{27}\zeta_3\right.\right. \\
& + 384\zeta_5 + \left(-\frac{352}{5}\zeta_2^2 + \frac{2144}{9}\zeta_2 + 352\zeta_3 - \frac{62012}{81}\right)L_{qr} + \left(\frac{352}{5}\zeta_2^2 - \frac{2144}{9}\zeta_2\right. \\
& + \frac{176}{3}\zeta_3 + \frac{980}{3}\left.)L_{fr} + \left(-\frac{176}{3}\zeta_2 + \frac{7120}{27}\right)L_{qr}^2 + \left(\frac{176}{3}\zeta_2 - \frac{7120}{27}\right)L_{fr}^2 + \left(-\frac{968}{27}\right)L_{qr}^3 + \left(\frac{968}{27}\right)L_{fr}^3 + \frac{594058}{729}\left.)C_A^2 C_F + \left(-\frac{32}{5}\zeta_2^2 + \frac{1648}{81}\zeta_2 + \frac{1808}{27}\zeta_3 + \left(-\frac{320}{9}\zeta_2 + \frac{16408}{81}\right)L_{qr} + \left(-\frac{32}{3}\zeta_2 + \frac{2312}{27}\right)L_{fr}^2 + \left(\frac{32}{3}\zeta_2 - \frac{2312}{27}\right)L_{qr}^2 + \left(\frac{320}{9}\zeta_2 - \frac{224}{3}\zeta_3 - \frac{1672}{27}\right)L_{fr} + \left(-\frac{352}{27}\right)L_{fr}^3 + \left(\frac{352}{27}\right)L_{qr}^3 - \frac{125252}{729}\right)C_A C_F n_f + \left(\frac{64}{5}\zeta_2^2\right.
\end{aligned}$$

$$\begin{aligned}
& -\frac{3584}{27}\zeta_2 + \frac{608}{9}\zeta_3 + \left(-\frac{2240}{9}\zeta_2 + \frac{640}{9}\zeta_3 + \frac{172}{9}\right)L_{fr} + \left(-\frac{256}{3}\zeta_2 + \frac{8}{3}\right)L_{qr}^2 \\
& + \left(\frac{256}{3}\zeta_2 + 56\right)L_{fr}^2 + \left(\frac{2240}{9}\zeta_2 - \frac{640}{9}\zeta_3 + \frac{92}{3}\right)L_{qr} + \left(-\frac{176}{3}\right)L_{qr}L_{fr} \\
& + \left(-32\right)L_{fr}^3 + \left(16\right)L_{qr}^2L_{fr} + \left(16\right)L_{qr}L_{fr}^2 - \frac{842}{9}C_F^2n_f + \left(-896\zeta_2\zeta_3\right. \\
& + \frac{25856}{27}\zeta_2 + 224\zeta_3 + \left(-\frac{2016}{5}\zeta_2^2 + \frac{15296}{9}\zeta_2 + \frac{5264}{9}\zeta_3 - \frac{4048}{9}\right)L_{fr} + \left(\frac{2016}{5}\zeta_2^2\right. \\
& - \frac{15296}{9}\zeta_2 - \frac{2240}{9}\zeta_3 + \frac{272}{3}\left.)L_{qr} + \left(-\frac{1120}{3}\zeta_2 + 192\zeta_3 - 344\right)L_{fr}^2 + \left(-96\zeta_2\right. \right. \\
& - 384\zeta_3 + \frac{920}{3}\left.)L_{qr}L_{fr} + \left(\frac{1408}{3}\zeta_2 + 192\zeta_3 + \frac{112}{3}\right)L_{qr}^2 + \left(-88\right)L_{qr}^2L_{fr} \\
& + \left(-88\right)L_{qr}L_{fr}^2 + \left(176\right)L_{fr}^3 - \frac{6464}{27}C_AC_F^2 + \left(\frac{64}{9}\zeta_3 + \left(-\frac{800}{81}\right)L_{qr} + \left(-\frac{160}{27}\right)L_{fr}^2\right. \\
& + \left(-\frac{32}{27}\right)L_{qr}^3 + \left(-\frac{32}{27}\right)L_{fr} + \left(\frac{32}{27}\right)L_{fr}^3 + \left(\frac{160}{27}\right)L_{qr}^2 \\
& + \frac{3712}{729}C_Fn_f^2 + \left(\left(-\frac{4416}{5}\zeta_2^2 + 256\zeta_2 + 480\zeta_3 - 128\right)L_{qr} + \left(\frac{4416}{5}\zeta_2^2 - 256\zeta_2\right. \right. \\
& - 480\zeta_3 + 128\left.)L_{fr} + \left(-576\zeta_2 - 384\zeta_3 + 168\right)L_{fr}^2 + \left(192\zeta_2 - 384\zeta_3\right)L_{qr}^2 \\
& + \left(384\zeta_2 + 768\zeta_3 - 168\right)L_{qr}L_{fr} + \left(-144\right)L_{qr}L_{fr}^2 + \left(144\right)L_{fr}^3\left.)C_F^3\right\} + g_{03},
\end{aligned} \tag{B.3}$$

C The Cusp and the soft anomalous dimensions

The quark cusp anomalous dimensions are given as [38],

$$A_1^{(b)} = C_F \left\{ 4 \right\}, \tag{C.1}$$

$$A_2^{(b)} = C_F \left\{ n_f \left(-\frac{40}{9} \right) + C_A \left(\frac{268}{9} - 8\zeta_2 \right) \right\}, \tag{C.2}$$

$$\begin{aligned}
A_3^{(b)} = C_F \left\{ n_f^2 \left(-\frac{16}{27} \right) + C_F n_f \left(-\frac{110}{3} + 32\zeta_3 \right) + C_A n_f \left(-\frac{836}{27} - \frac{112}{3}\zeta_3 + \frac{160}{9}\zeta_2 \right) \right. \\
\left. + C_A^2 \left(\frac{490}{3} + \frac{88}{3}\zeta_3 - \frac{1072}{9}\zeta_2 + \frac{176}{5}\zeta_2^2 \right) \right\}, \tag{C.3}
\end{aligned}$$

The four loops coefficient [39–44] is also known numerically and the perturbative series for $A^{(b)}$ finally looks like

$$\begin{aligned}
A^{(b)}(n_f=3) &= 0.42441 \alpha_s (1 + 0.7266 \alpha_s + 0.7341 \alpha_s^2 + 0.665 \alpha_s^3 + \dots), \\
A^{(b)}(n_f=4) &= 0.42441 \alpha_s (1 + 0.6382 \alpha_s + 0.5100 \alpha_s^2 + 0.317 \alpha_s^3 + \dots), \\
A^{(b)}(n_f=5) &= 0.42441 \alpha_s (1 + 0.5497 \alpha_s + 0.2840 \alpha_s^2 + 0.013 \alpha_s^3 + \dots).
\end{aligned}$$

$$(C.4)$$

$$D_1^{(b)} = C_F \left\{ 0 \right\}, \quad (C.5)$$

$$D_2^{(b)} = C_F \left\{ n_f \left(\frac{112}{27} - \frac{16}{3} \zeta_2 \right) + C_A \left(-\frac{808}{27} + 28 \zeta_3 + \frac{88}{3} \zeta_2 \right) \right\}, \quad (C.6)$$

$$D_3^{(b)} = C_F \left\{ n_f^2 \left(-\frac{1856}{729} + \frac{160}{27} \zeta_3 + \frac{320}{27} \zeta_2 \right) + C_F n_f \left(\frac{1711}{27} - \frac{304}{9} \zeta_3 - 16 \zeta_2 - \frac{32}{5} \zeta_2^2 \right) \right. \\ \left. + C_A n_f \left(\frac{62626}{729} - \frac{1240}{9} \zeta_3 - \frac{14696}{81} \zeta_2 + \frac{368}{15} \zeta_2^2 \right) + C_A^2 \left(-\frac{297029}{729} - 192 \zeta_5 \right. \right. \\ \left. \left. + \frac{20072}{27} \zeta_3 + \frac{49112}{81} \zeta_2 - \frac{176}{3} \zeta_2 \zeta_3 - \frac{1496}{15} \zeta_2^2 \right) \right\}, \quad (C.7)$$

References

- [1] ATLAS collaboration, G. Aad et al., *Observation of a new particle in the search for the Standard Model Higgs boson with the ATLAS detector at the LHC*, *Phys. Lett.* **B716** (2012) 1 [1207.7214].
- [2] CMS collaboration, S. Chatrchyan et al., *Observation of a new boson at a mass of 125 GeV with the CMS experiment at the LHC*, *Phys. Lett.* **B716** (2012) 30 [1207.7235].
- [3] LHC HIGGS CROSS SECTION WORKING GROUP collaboration, J. R. Andersen et al., *Handbook of LHC Higgs Cross Sections: 3. Higgs Properties*, 1307.1347.
- [4] LHC HIGGS CROSS SECTION WORKING GROUP collaboration, D. de Florian et al., *Handbook of LHC Higgs Cross Sections: 4. Deciphering the Nature of the Higgs Sector*, 1610.07922.
- [5] ATLAS COLLABORATION collaboration, *Combined measurements of Higgs boson production and decay using up to 80 fb⁻¹ of proton–proton collision data at $\sqrt{s} = 13$ TeV collected with the ATLAS experiment*, Tech. Rep. ATLAS-CONF-2019-005, CERN, Geneva, Mar, 2019.
- [6] CMS collaboration, A. M. Sirunyan et al., *Combined measurements of Higgs boson couplings in proton–proton collisions at $\sqrt{s} = 13$ TeV*, Submitted to: *Eur. Phys. J.* (2018) [1809.10733].
- [7] C. Englert, O. Mattelaer and M. Spannowsky, *Measuring the Higgs–bottom coupling in weak boson fusion*, *Phys. Lett.* **B756** (2016) 103 [1512.03429].
- [8] J. F. Gunion, H. E. Haber, G. L. Kane and S. Dawson, *The Higgs hunter’s guide*, (Addison-Wesley, Menlo Park, 1990)., .
- [9] S. Dittmaier, M. Krmer and M. Spira, *Higgs radiation off bottom quarks at the Tevatron and the CERN LHC*, *Phys. Rev.* **D70** (2004) 074010 [hep-ph/0309204].
- [10] S. Dawson, C. B. Jackson, L. Reina and D. Wackeroth, *Exclusive Higgs boson production with bottom quarks at hadron colliders*, *Phys. Rev.* **D69** (2004) 074027 [hep-ph/0311067].
- [11] M. Wiesemann, R. Frederix, S. Frixione, V. Hirschi, F. Maltoni and P. Torrielli, *Higgs production in association with bottom quarks*, *JHEP* **02** (2015) 132 [1409.5301].

- [12] C. Duhr, F. Dulat and B. Mistlberger, *Higgs production in bottom-quark fusion to third order in the strong coupling*, [1904.09990](#).
- [13] D. Dicus, T. Stelzer, Z. Sullivan and S. Willenbrock, *Higgs boson production in association with bottom quarks at next-to-leading order*, *Phys. Rev.* **D59** (1999) 094016 [[hep-ph/9811492](#)].
- [14] C. Balazs, H.-J. He and C. P. Yuan, *QCD corrections to scalar production via heavy quark fusion at hadron colliders*, *Phys. Rev.* **D60** (1999) 114001 [[hep-ph/9812263](#)].
- [15] R. V. Harlander and W. B. Kilgore, *Higgs boson production in bottom quark fusion at next-to-next-to leading order*, *Phys. Rev.* **D68** (2003) 013001 [[hep-ph/0304035](#)].
- [16] V. Ravindran, *Higher-order threshold effects to inclusive processes in QCD*, *Nucl. Phys.* **B752** (2006) 173 [[hep-ph/0603041](#)].
- [17] T. Ahmed, N. Rana and V. Ravindran, *Higgs boson production through $b\bar{b}$ annihilation at threshold in N^3LO QCD*, *JHEP* **10** (2014) 139 [[1408.0787](#)].
- [18] M. Bonvini, A. S. Papanastasiou and F. J. Tackmann, *Matched predictions for the $b\bar{b}H$ cross section at the 13 TeV LHC*, *JHEP* **10** (2016) 053 [[1605.01733](#)].
- [19] S. Forte, D. Napoletano and M. Ubiali, *Higgs production in bottom-quark fusion in a matched scheme*, *Phys. Lett.* **B751** (2015) 331 [[1508.01529](#)].
- [20] M. A. Ebert, J. K. L. Michel and F. J. Tackmann, *Resummation Improved Rapidity Spectrum for Gluon Fusion Higgs Production*, *JHEP* **05** (2017) 088 [[1702.00794](#)].
- [21] G. F. Sterman, *Summation of Large Corrections to Short Distance Hadronic Cross-Sections*, *Nucl. Phys.* **B281** (1987) 310.
- [22] S. Catani and L. Trentadue, *Resummation of the QCD Perturbative Series for Hard Processes*, *Nucl. Phys.* **B327** (1989) 323.
- [23] S. Catani and L. Trentadue, *Comment on QCD exponentiation at large x* , *Nucl. Phys.* **B353** (1991) 183.
- [24] C. Anastasiou, C. Duhr, F. Dulat, F. Herzog and B. Mistlberger, *Higgs Boson Gluon-Fusion Production in QCD at Three Loops*, *Phys. Rev. Lett.* **114** (2015) 212001 [[1503.06056](#)].
- [25] C. Anastasiou, C. Duhr, F. Dulat, E. Furlan, T. Gehrmann, F. Herzog et al., *High precision determination of the gluon fusion Higgs boson cross-section at the LHC*, *JHEP* **05** (2016) 058 [[1602.00695](#)].
- [26] M. Bonvini and S. Marzani, *Resummed Higgs cross section at N^3LL* , *JHEP* **09** (2014) 007 [[1405.3654](#)].
- [27] M. Bonvini, S. Marzani, C. Muselli and L. Rottoli, *On the Higgs cross section at N^3LO+N^3LL and its uncertainty*, *JHEP* **08** (2016) 105 [[1603.08000](#)].
- [28] M. Bonvini and L. Rottoli, *Three loop soft function for N^3LL' gluon fusion Higgs production in soft-collinear effective theory*, *Phys. Rev.* **D91** (2015) 051301 [[1412.3791](#)].
- [29] T. Gehrmann and D. Kara, *The $Hb\bar{b}$ form factor to three loops in QCD*, *JHEP* **09** (2014) 174 [[1407.8114](#)].
- [30] T. Ahmed, M. Mahakhud, N. Rana and V. Ravindran, *Drell-Yan Production at Threshold to Third Order in QCD*, *Phys. Rev. Lett.* **113** (2014) 112002 [[1404.0366](#)].

- [31] S. Catani, D. de Florian, M. Grazzini and P. Nason, *Soft gluon resummation for Higgs boson production at hadron colliders*, *JHEP* **07** (2003) 028 [[hep-ph/0306211](#)].
- [32] S. Moch, J. A. M. Vermaseren and A. Vogt, *Higher-order corrections in threshold resummation*, *Nucl. Phys.* **B726** (2005) 317 [[hep-ph/0506288](#)].
- [33] R. V. Harlander, S. Liebler and H. Mantler, *SusHi: A program for the calculation of Higgs production in gluon fusion and bottom-quark annihilation in the Standard Model and the MSSM*, *Comput. Phys. Commun.* **184** (2013) 1605 [[1212.3249](#)].
- [34] S. Catani, M. L. Mangano, P. Nason and L. Trentadue, *The Resummation of soft gluons in hadronic collisions*, *Nucl. Phys.* **B478** (1996) 273 [[hep-ph/9604351](#)].
- [35] L. A. Harland-Lang, A. D. Martin, P. Motylinski and R. S. Thorne, *Parton distributions in the LHC era: MMHT 2014 PDFs*, *Eur. Phys. J.* **C75** (2015) 204 [[1412.3989](#)].
- [36] A. Buckley, J. Ferrando, S. Lloyd, K. Nordström, B. Page, M. Rfenacht et al., *LHAPDF6: parton density access in the LHC precision era*, *Eur. Phys. J.* **C75** (2015) 132 [[1412.7420](#)].
- [37] A. Accardi et al., *A Critical Appraisal and Evaluation of Modern PDFs*, *Eur. Phys. J.* **C76** (2016) 471 [[1603.08906](#)].
- [38] S. Moch, J. A. M. Vermaseren and A. Vogt, *The Three loop splitting functions in QCD: The Nonsinglet case*, *Nucl. Phys.* **B688** (2004) 101 [[hep-ph/0403192](#)].
- [39] S. Moch, B. Ruijl, T. Ueda, J. A. M. Vermaseren and A. Vogt, *On quartic colour factors in splitting functions and the gluon cusp anomalous dimension*, *Phys. Lett.* **B782** (2018) 627 [[1805.09638](#)].
- [40] R. N. Lee, A. V. Smirnov, V. A. Smirnov and M. Steinhauser, *The n_f^2 contributions to fermionic four-loop form factors*, *Phys. Rev.* **D96** (2017) 014008 [[1705.06862](#)].
- [41] A. Grozin, *Four-loop cusp anomalous dimension in QED*, *JHEP* **06** (2018) 073 [[1805.05050](#)].
- [42] J. M. Henn, T. Peraro, M. Stahlhofen and P. Wasser, *Matter dependence of the four-loop cusp anomalous dimension*, [1901.03693](#).
- [43] R. N. Lee, A. V. Smirnov, V. A. Smirnov and M. Steinhauser, *Four-loop quark form factor with quartic fundamental colour factor*, *JHEP* **02** (2019) 172 [[1901.02898](#)].
- [44] A. von Manteuffel and R. M. Schabinger, *Quark and gluon form factors in four loop QCD: the N_f^2 and $N_{q\gamma}N_f$ contributions*, [1902.08208](#).